Heat Storage in Urban Areas: Local-Scale Observations and Evaluation of a Simple Model

C. S. B. GRIMMOND

Climate and Meteorology Program, Department of Geography, Indiana University, Bloomington, Indiana

T. R. OKE

Atmospheric Science Program, Department of Geography, University of British Columbia, Vancouver, British Columbia, Canada

(Manuscript received 25 June 1998, in final form 30 September 1998)

ABSTRACT

The flux density of sensible heat to or from storage in the physical mass of the city is determined for seven cities (Chicago, Illinois; Los Angeles, California; Mexico City, Distrito Federal; Miami, Florida; Sacramento, California; Tucson, Arizona; and Vancouver, British Columbia) in North America across a 30° latitudinal range. These cities have a variety of synoptic-scale climates and surface cover and structural morphologies. In all cases the ''measured'' storage heat flux is determined as the energy balance residual from direct observations of net all-wave radiation, and sensible and latent heat fluxes conducted using the same radiometer and eddy correlation techniques. Databases describing the surface characteristics around each site are developed from analysis of aerial photography and field surveys. Results indicate that storage heat flux is a significant component of the surface energy balance at all sites and is greatest at downtown and light industrial sites. Hysteresis behavior, of varying degrees, is seen at all locations. A simple objective hysteresis model (OHM), which calculates storage heat flux as a function of net all-wave radiation and the surface properties of the site, is found to perform well in the mean for most cases, with the notable exception of Tucson; but considerable scatter is observed at some sites. Some of this is attributed to the moisture, wind, and synoptic controls at each of the sites, and to hour-to-hour variability in the convective fluxes that the OHM does not simulate. Averaging over 2 to 3 h may be a more appropriate way to use the model. Caution should be used when employing the OHM in windy environments.

1. Introduction

In urban areas, the storage heat flux (ΔQ_S) is the net uptake or release of energy (per unit area and time) by sensible heat changes in the urban canopy air layer, buildings, vegetation, and the ground. The area referred to here is part of the imaginary horizontal surface at the top of a ''box'' that extends from just above roof level to the depth below the city where the net vertical heat flux is zero on a daily basis (c.f. Oke 1988). Knowledge of the storage heat flux term is required in a variety of applications; for example, to model evapotranspiration, sensible heat flux, boundary layer growth, etc. Furthermore, the thermal inertia provided by this storage term is often regarded as a key process in the genesis of urban heat islands. Given the materials and morphology of the urban surface, it is widely recognized that heat storage in urban areas will be more significant than at simpler bare soil or agricultural sites. However, ΔQ_S is difficult to measure or model because of the complex three-dimensional structure of the urban surface and the diversity of material types of which the urban interface is composed.

The objectives of this paper are twofold. First, to examine empirically the storage heat flux for seven urban areas within Canada, the United States, and Mexico. These cities were selected to represent a range of latitudes, synoptic-scale climates, surface cover, and structural morphologies. The observations were taken in suburban, light industrial, and urban ''downtown'' land use areas (see Table 1). Second, to evaluate the performance of the Grimmond et al. (1991) objective hysteresis model (OHM), which calculates the storage heat flux as a function of net all-wave radiation and the surface properties of the site. To date, this simple model has been evaluated only in Vancouver, the city for which it was initially developed (Grimmond et al. 1991; Roth and Oke 1994).

Corresponding author address: Dr. C. S. Grimmond, Climate and Meteorology Program, Department of Geography, Indiana University, Bloomington, IN 47405.
E-mail: grimmon@indiana.edu

TABLE 1. Study sites and measurement periods ordered by decreasing fraction of the surface cover built (combined area of roofs, impervious ground and walls) (or conversely increasing area that is vegetated). Code refers to the location and year of the observations, for example, ME93 refers to Mexico City in 1993. General land-use classes are: Urb—urban "downtown"; Sub—suburban residential; LI—light industrial. UTZ—Urban terrain zones according to Ellefsen (1985). Fractions of surface cover (A_V, A_R, A_I, A_W) defined in text.

Site	Code	Lat./long. of site	Wind directions analyzed	Observation period	Land use	UTZ	Fractions of surface cover				
							A_V	A_R	A_I	A_W	A_C/A_P
Mexico City, D.F.	Me93	19°26′N 99°08′W	0–180	Dec 1993	Urb	A2	0.01	0.32	0.25	0.42	1.75
Vancouver, BC	Vl92	49°16′N 123°06′W	0–360	Aug 1992	LI	Do4	0.04	0.37	0.32	0.27	1.39
Chicago, IL	C95	41°57′N 87°48′W	180–360	Jun–Aug 1995	Sub	Dc3	0.24	0.23	0.14	0.38	1.71
Miami, FL	Mi95	25°44′N 80°22′W	24–170	May–Jun 1995	Sub	Do3	0.26	0.29	0.24	0.21	1.33
Tucson, AZ	T90	32°07′N 110°56′W	315–45; 135–270	Jun 1990	Sub	Do3	0.28	0.19	0.33	0.20	1.25
San Gabriel, LA, CA	Sg94	34°05′N 118°05′W	0–360	Jul 1994	Sub	Do3	0.31	0.26	0.26	0.14	1.18
Vancouver, BC*	Vs92	49°15′N 123°18′W	135–305, 345–90	Jul–Sep 1992	Sub	Dc3	0.33	0.22	0.17	0.29	1.42
Sacramento, CA	S91	38°39′N 121°30′W	0–360	Aug 1991	Sub	Do3	0.42	0.30	0.10	0.15	1.22
Arcadia, LA, CA	A94	34°08′N 118°03′W	180–360	Jul 1994	Sub	Do3	0.47	0.22	0.17	0.12	1.17
Arcadia, LA, CA	A93	34°08′N 118°03′W	180–360	Jul–Aug 1993	Sub	Do3	0.49	0.21	0.16	0.12	1.16

* Location and surface cover same as in Vs89 study.

2. Study sites

The neighborhoods studied lie within the metropolitan areas of: Chicago, Illinois; Los Angeles, California; Mexico City, Distrito Federal; Miami, Florida; Sacramento, California; Tucson, Arizona; and Vancouver, British Columbia (Table 1). Each set of observations is identified by its location (one or two letter code) and the year in which it was conducted (see list of codes in Table 1). The field sites are predominantly residential with detached one- to two-story houses, and vegetation (trees, shrubs, grass) surrounding the buildings. Two exceptions are the downtown site in Mexico City (Me93), with the tallest buildings/deepest urban canyons (buildings on average have 4–5 stories), and a light industrial area in Vancouver (V192), with one- and two-story warehouse-type structures. Both of these areas have scant vegetation. All observations were undertaken during the spring–summertime period, with the exception of Mexico City where measurements were conducted in the dry season of December 1993 (Table 1). Simultaneous observations were made at two different locations within both Los Angeles (A94 and Sg94) and Vancouver (Vs92 and Vl92). In addition, data were collected at the same site in Los Angeles during two consecutive summers (A93 and A94).

For each of the sites, geographic information systems (GIS) containing surface descriptors have been developed from aerial photographs and field surveys, using procedures similar to those discussed by Grimmond and Souch (1994), and Grimmond (1996). These allow surface characteristics (materials, morphology, height, etc., of the building and vegetative fractions) to be calculated for areas of varying size and shape around each measurement site. In this paper each measurement site is characterized in terms of 1) the plan-area vegetated (trees, grass, etc.); 2) the plan-area impervious (concrete/asphalt/gravel parking lots, roads, sidewalks, etc. but not buildings); and 3) the three-dimensional surface area of the buildings, subdivided into the area of roofs and walls. Thus the total surface area (A_C) is defined as

$$A_C = A_V + A_I + A_R + A_W, \quad (1)$$

where A_V is the plan-area vegetated, A_I the plan area of impervious ground, A_R the area of roofs, and A_W the surface area of walls. The ratio A_C to A_P total (plan area) is a measure of the three-dimensional morphology of the site. The presence of parks, commercial areas, schools, and differences in houses and their gardens result in variations in surface cover around each measurement site; thus fetch characteristics may differ depending on wind direction. In order to identify potential relationships between fluxes and surface cover, it is critical that the fluxes representative of source areas with different surface properties are not averaged together. Using the air photographs and databases for each site, directions with reasonably homogeneous fetch (areas with no significant changes in building/vegetation di-

mensions and density) were identified (listed in Table 1). Only fluxes from these directions are considered here, unless otherwise noted.

Source areas for the hourly convective flux measurements (described below) were calculated using the FSAM model of Schmid (1994, 1997). The average areas of these source areas are of the order of 10^4 m^2 in the middle of the day, 10^6 m^2 in the early morning and evening. FSAM source weight functions were then overlain on the georeferenced database, as described by Grimmond and Souch (1994), and the surface characteristics for each hour of measurements determined. The average surface cover for the hourly source areas are shown in Table 1. Given that meteorological conditions differed slightly in 1993 and 1994 at Arcadia, even though it was almost the same measurement location, source areas, and thus average surface cover, are slightly different.

In Table 1 the cities are ordered by decreasing area built/increasing plan-area vegetated. Here, A_V has the greatest range of any of the surface cover types considered. Values extend from 1% at the downtown site (Me93) and 4% at the light industrial site (Vl92), to 42% in Sacramento and 49% in Arcadia (A93). Most of the suburban values cluster between 24% and 33%. The surface area of the walls is the most important surface fraction in Mexico City (43%), a consequence of the tall, closely spaced buildings of the downtown site. In many of the suburbs the fractions of the surface area covered by impervious surfaces and roofs are approximately similar (both 15%–35%). Notable exceptions are Tucson [where impervious ground surfaces are more important because of wide roads relative to small houses and gardens with xeriscape or zeroscape (devoid of vegetation) style of landscaping] and Sacramento (where impervious surfaces are fairly insignificant and roofs are more important). The total surface to plan area ratio (A_C/A_P) ranges from 1.16 in Arcadia to 1.75 in Mexico City. Further surface geometric characteristics of these sites are given in Grimmond and Oke (1999a).

3. Observation methods

All measurements were conducted in the framework of the surface energy balance (see a full description of its application to urban areas in Oke 1988). At each site, instruments were mounted on tall towers and measurements were made in the constant flux layer of the urban boundary layer (Oke et al. 1989), and are representative of the local-scale (horizontal length scale 10^2–10^4 m).

In all cases, net all-wave radiation was measured using either Swissteco (model S1) or REBS net pyrradiometers (model Q*6) and the turbulent sensible and latent heat fluxes were measured directly using the eddy correlation approach. The fast response instruments, mounted less than 0.15 m apart, consisted of a Campbell Scientific Inc (CSI) one-dimensional sonic anemometer and fine wire thermocouple system (model CA27) to measure the fluctuations of vertical wind velocity and temperature, and a CSI krypton hygrometer (model KH20) to measure those of absolute humidity. The vertical wind velocity, air temperature, and humidity fluctuations were sampled at 5 or 10 Hz. Covariances were determined for 15-min periods. Flux corrections were made for oxygen absorption and air density (Webb et al. 1980; Tanner and Greene 1989; Tanner et al. 1993). No corrections were made for frequency response or spatial separation of the sensors. All times reported are local mean solar time [local apparent time (LAT)].

The ''measured'' storage heat flux (ΔQ_S) is determined as the energy balance residual from direct observation of net all-wave radiation (Q*), and the convective sensible (Q_H) and latent heat (Q_E) fluxes

$$\Delta Q_S = Q^* - (Q_H + Q_E). \quad (2)$$

This has the inherent problem that all measurement errors of the other energy balance fluxes are accumulated in the ΔQ_S term. These errors include those introduced due to spatial inconsistency of the energy balances, which arise because the source area of the turbulent fluxes varies (as a sensitive function of wind direction, atmospheric stability, and surface roughness), whereas for the radiant fluxes it is fixed in time (Schmid et al. 1991).

Additional error is introduced into the residual ΔQ_S because neither the anthropogenic heat flux due to combustion (Q_F) nor horizontal advection (ΔQ_A) are included. The magnitude of Q_F depends on the nature and spatial pattern of sources. In residential areas, the most notable sources are major roads and large nonresidential stationary sources (e.g., strip malls with energy intensive users) (Grimmond 1992). Here, Q_F enters the climate system as radiation (from warmer surfaces), as sensible heat convected into the air from warmer surfaces, sensible or latent heat flux convected directly from tail pipes, chimneys or leakage from buildings, or from sensible heat conducted to storage. The radiative and convective portions are sensed by the instruments, thus only that portion temporarily sequestered in building fabric contributes to ΔQ_S. This also highlights the fact that Eq. (2) is a statement of the *measured* energy balance (i.e., the terms are defined by the instrument systems not just theory). It is important to note that in theoretical and/or numerical modeling studies of the urban energy balance, Q_F must be included explicitly as an energy source.

The impact of ΔQ_A on ΔQ_S obtained by residual is more difficult to generalize because it depends on the position of the site relative to the direction of the regionally generated flow and the distance from the contrasting surfaces. All the cities studied here experience some form of mesoscale circulation; however, in all cases, sites were selected to minimize this effect, so that the impact on the ΔQ_S values probably are small. An order of magnitude of this effect can be obtained from the analysis of Steyn (1985). He demonstrates for the

TABLE 2. Daily (24-h) and daytime ($Q^* > 0$ W m^{-2}) mean observed fluxes and ratios of fluxes under all types of sky conditions when at 30 min past the hour the wind direction was within acceptable limits. See Table 1 for site codes. Data in both parts of the table ordered by significance of ΔQ_S to the energy balance (i.e., Λ). Daytime n the number of hours within each day that $Q^* > 0$ W m^{-2}; Daily n total number of hours analyzed.

	Fluxes (MJ m^{-2} d^{-1})				Ratios					
	Q^*	Q_H	Q_E	ΔQ_S	Q_H/Q_E β	Q_H/Q^* χ	Q_E/Q^* Υ	$\Delta Q_S/Q^*$ Λ	$Q_H/\Delta Q_S$ κ	n
Daytime ($Q^* > 0$ W m^{-2})										
Me93	8.71	3.34	0.34	5.03	9.85	0.38	0.04	0.58	0.66	10
Vl92	13.95	5.90	1.34	6.71	4.42	0.42	0.10	0.48	0.88	13
A94	17.49	7.43	4.61	5.45	1.61	0.43	0.26	0.31	1.37	13
Mi95	15.97	6.76	4.38	4.84	1.55	0.42	0.27	0.30	1.40	13
A93	15.44	5.96	4.79	4.69	1.24	0.39	0.31	0.30	1.27	13
Sg94	14.65	7.13	3.28	4.25	2.17	0.49	0.22	0.29	1.68	13
S91	12.66	5.25	4.16	3.26	1.26	0.41	0.33	0.26	1.61	12
T90	16.35	8.49	4.08	3.78	2.08	0.52	0.25	0.23	2.24	12
C95	16.86	7.74	6.24	2.88	1.24	0.46	0.37	0.17	2.69	13
Vs92	12.13	7.50	2.62	2.01	2.87	0.62	0.22	0.17	3.73	14
Daily (24 h)										
Vl92	11.41	5.98	1.48	3.95	4.05	0.52	0.13	0.35	1.51	313
A94	15.58	7.50	4.70	3.38	1.60	0.48	0.30	0.22	2.22	350
A93	13.74	5.99	4.93	2.82	1.21	0.44	0.36	0.21	2.12	588
Mi95	13.74	6.69	4.58	2.49	1.47	0.49	0.33	0.18	2.69	209
Sg94	12.45	7.36	3.46	1.63	2.13	0.59	0.28	0.13	4.52	468
S91	9.72	4.98	4.38	0.35	1.14	0.51	0.45	0.04	15.15	223
C95	14.89	7.56	6.80	0.53	1.11	0.51	0.46	0.04	14.17	174
T90**	12.50	7.73	4.90	−0.12	1.58	0.62	0.39	−0.01	−61.95	131
Vs92	8.88	7.28	2.68	−1.09	2.72	0.82	0.30	−0.12	−6.70	572
Me93*	3.38	3.61	0.31	−0.54	11.58	1.07	0.09	−0.16	−6.73	81

* Missing hours (at 2, 6) linearly interpolated.
** Missing hours (at 0, 1, 2, 22, 23) linearly interpolated.

Vancouver suburban site (Vs), where there is a sea breeze circulation, that advection is small (for all hours 2.5 W m^{-2}; values are larger when individual time periods are considered but still <16 W m^{-2} at the maximum).

4. Observed average energy balance characteristics

To provide context for comparison of the storage heat fluxes for the respective cities, the mean energy balance fluxes for each city are presented for all-sky conditions (Table 2). These data are the average fluxes from the directions listed in Table 1. In addition, five ratios are considered: the three fluxes normalized by the available radiant energy ($\chi = Q_H/Q^*$, $\Upsilon = Q_E/Q^*$, and $\Lambda = \Delta Q_S/Q^*$); Bowen ratio of the convective fluxes ($\beta = Q_H/Q_E$); and the ratio of the sensible heat fluxes to the atmosphere and the substrate ($\kappa = Q_H/\Delta Q_S$).

Complete details of the energy balances observed at each site are not given here. See Grimmond and Oke (1995) for discussion of data collected in Tucson, Sacramento, and Arcadia 1993; Grimmond et al. (1996) for Arcadia and San Gabriel; King and Grimmond (1997) for Chicago 1995; Oke et al. (1999) for Mexico City; and Oke et al. (1999) for Vancouver. The discussion here emphasizes average flux partitioning.

Before interpreting these data, it is important to recall that in all of the cities, except Mexico City, observations were conducted in the spring or summer. This influences both the size of the fluxes and also the number of hours each day when Q^* is greater than zero (Table 2).

In absolute terms, the daily (24 h) storage heat flux is greatest at the Vancouver light industrial site and lowest at the Vancouver suburban site (excluding the winter results of Mexico City) (Table 2). For daytime ($Q^* > 0$) hours only, ΔQ_S remains greatest and lowest at the same two sites, although the ordering of the other cities between them changes slightly. As expected, in summertime there is a net gain of energy at the surface for all sites except Vs92 and T90. However, the magnitudes of the gain over a daily period documented here at some of the sites are surprisingly large (Table 2). The size of the net gain (24 h Λ) is approximately ranked according to the size of the daytime ΔQ_S and Λ. This indicates a proportionate error and suggests it is related, at least in part, to cumulative measurement errors. In Mexico City, a net-loss at the surface was documented, as expected for wintertime.

When the daytime data are normalized by net all-wave radiation, it is evident that the storage heat flux is a very important term in the surface energy balance (Table 2); ΔQ_S ranges from 17% to 58% of Q^*. At the ''downtown'' site (Me93) ΔQ_S is the most significant flux ($\Lambda_{urb} = 0.58$), at the light industrial site the ratio is slightly smaller, ($\Lambda_{LI} = 0.48$) but still the largest single

flux, while at the suburban sites Λ varies between 0.17 and 0.31 (median value 0.275). Therefore, in general, in the more urban or built-up areas (sites with more impervious surfaces) a greater proportion of the energy goes into warming the urban fabric. Among the suburban sites there is no simple relationship between Λ_{sub} and any of the single measures of surface cover. Relatively, the storage heat flux is most important in Arcadia 1994, followed closely by Miami, San Gabriel, Arcadia (1993), and Sacramento. It is least important in Tucson, Chicago, and Vancouver; however, in these cities it still accounts for approximately one-fifth of the daytime radiant surplus.

At the central urban and light industrial sites the daytime latent heat fluxes are much smaller than the storage heat fluxes (Table 2). This is to be expected because these sites have very small fractions of vegetation cover (Table 1) (Me93 $\Upsilon_{urb} = 0.04$ $A_V = 1\%$; V192 $\Upsilon_{LI} = 0.10$ $A_V = 4\%$). At the suburban sites the median Υ_{sub} is 0.27 (range 0.22–0.37). Here, Υ is of the same order as Λ (± 0.05) at all the other suburban residential sites except C95 where Υ is 0.37 and Λ only 0.17. During the summer of 1995 record temperatures were experienced in Chicago (NOAA 1995). During this period no limitations were imposed on external water use and extensive irrigation was observed. This resulted in very high evaporation rates; in absolute terms daytime Q_E is 1.51 MJ m^{-2} d^{-1} greater than any other site. The smallest suburban value ($\Upsilon = 0.22$) was for Vancouver in 1992. The Vs92 observations were conducted during an extended period with no rainfall, and there was a ban on outdoor water use (Oke et al. 1999). Consequently the suburban system had little water available. Data collected at the same site in 1989 (Roth and Oke 1994) yield a value for Υ of 0.30. For the other suburban sites, where there was no rainfall, but regular irrigation, Υ does not correlate simply with the area vegetated; however, it is important to note that in these cities (A93, A94, Mi95, S91, Sg94) in the summertime Υ varies only over a very small range.

Differences in the absolute magnitude and relative significance of the sensible heat flux among the urban, light industrial, and suburban residential land uses are not obvious. As a fraction of the radiant energy (χ), the sensible heat flux for the two nonsuburban sites ($\chi_{urb} = 0.38$, $\chi_{LI} = 0.42$) fall at the lower end of the range for the suburban sites ($\chi_{sub} = 0.39$–0.62; median $\chi_{sub} = 0.45$). Values are much higher for Vancouver than any other site (0.10 greater than the next city Tucson), but this is related to the absence of irrigation in 1992, and the very low values of Q_E are not typical for that city (Oke et al. 1999).

In all cities, daytime and daily β values are greater than unity, indicating that more energy is going into heating the air than evaporating water. For suburban areas, the daytime range is 1.37–2.87. The highest suburban value for the anomalously dry Vs92 is 2.87; this was still significantly less than that of the light industrial ($\beta_{LI} = 4.42$) and urban ($\beta_{urb} = 9.85$) sites. Thus, convective flux partitioning shows the expected spatial variation between land uses during the daytime. Again, among the suburban sites there is no simple relationship between β and any simple measure of surface cover.

Similarly the partitioning of the sensible heat fluxes between the air and the surface fabric (κ) does not show a simple relation to measures of surface cover. This is not unexpected given the variability of the sensible heat flux and the fact that ΔQ_S contains the residual measurement error. When κ is greater than 1, the atmosphere dissipates a greater portion of the radiant energy than is stored; when it is less than 1 the surface fabric is a more effective sink. At all suburban sites, κ is greater than 1; while the light industrial and urban sites have daytime κ values less than 1. At all sites, except the atypical Vs92, daytime κ is less than the value of 3.3 suggested by Stull (1988) for rural environments, thereby confirming the general notion that cities are relative stores of sensible heat.

Similarity of flux partitioning between different years is evident in the results for Arcadia where observations were made in both 1993 and 1994. Although there are differences in the magnitudes of the absolute fluxes for Arcadia for the two years (A93 was cloudier in the mornings than A94), all of the Q^* normalized flux ratios are very similar (less than 5% variation) (Table 2). Notably Λ is almost identical in the two years, both in the daytime and over 24-h periods. The κ ratio also is very stable ($\kappa_{A93} = 1.37$, $\kappa_{A94} = 1.27$).

5. Observed diurnal storage heat flux characteristics

The average diurnal variation of ΔQ_S for each of the sites and cities (Fig. 1) show remarkable similarity in their pattern and magnitude. These figures are drawn so that the time when Q^* becomes positive in the morning and negative in the late evening are coincident for each site; that is, the effects of differences in day length are removed. The portion of the timescale from 0 to 1 represents whatever period the site experiences net radiative surplus (''daytime''), and from 1 to 2 the period of deficit.

Given that ΔQ_S is a residual term, it is encouraging to see that its course (Fig. 1a) is relatively smooth and similar to that of other systems such as soils, crops, and forests, where direct measurement is possible (e.g., Oke 1987; Stull 1988). On the other hand, the magnitude of ΔQ_S is considerably larger than for most natural systems, except water. The average peak daytime values of 150–300 W m^{-2} are about 2–6 times greater than such systems. When normalized by the net radiation (as Λ) the relative ordering of cities (and sites) in terms of the importance of storage uptake and release in their energy balance becomes clear (Fig. 1b). The most heavily developed and least vegetated Me93 and Vl92 sites are the largest daytime stores. Both sites plot distinctly

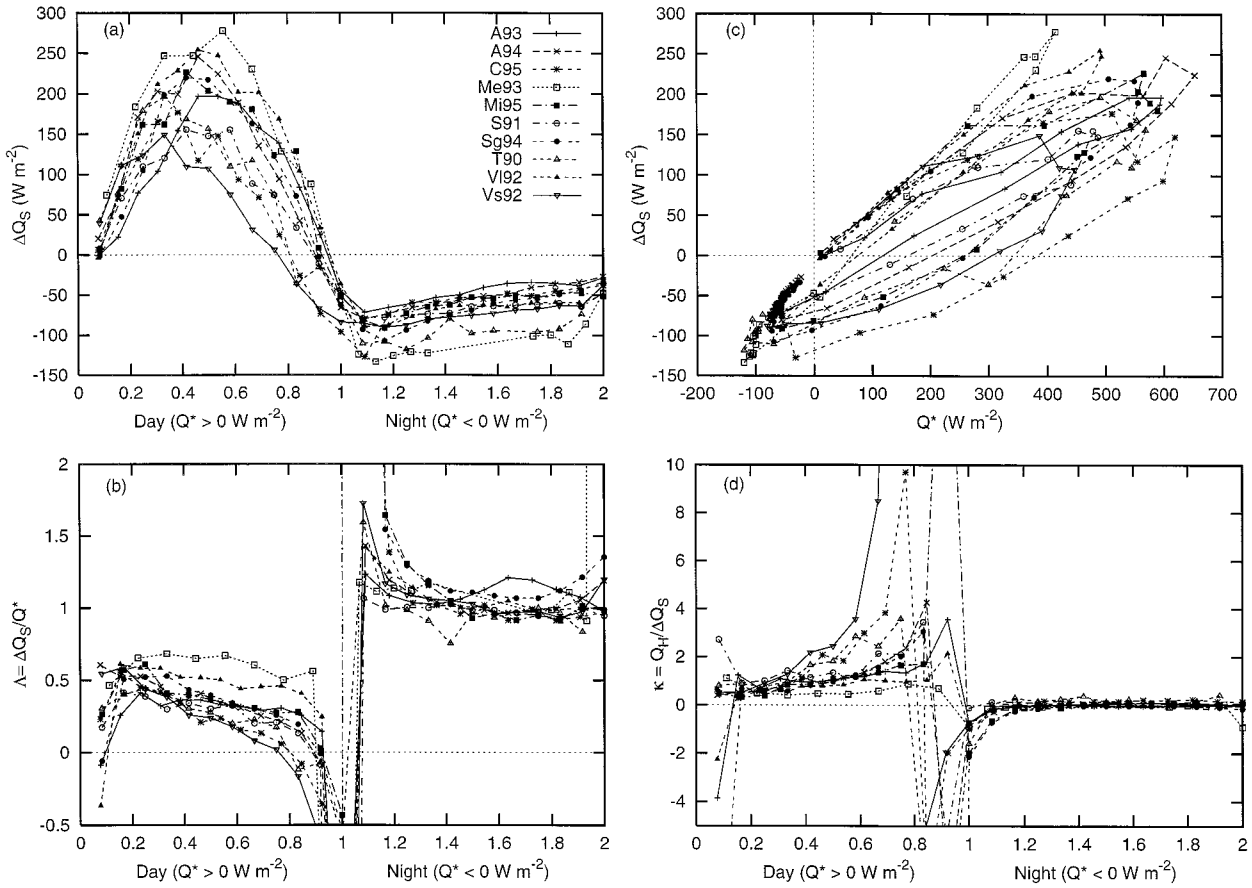

FIG. 1. Mean diurnal patterns of observed (a) ΔQ_S (W m^{-2}), (b) $\Delta Q_S/Q^*$, (c) ΔQ_S vs Q^*, and (d) $Q_H/\Delta Q_S$ for each of the datasets (see details in Table 1).

above the suburban values. The latter show a range but are clustered together.

When individual hourly values are plotted for each day (Fig. 2) it is evident that the residual fluxes are quite variable from hour to hour, and at some of the sites (notably Sacramento and Chicago) from day to day. Some of the day-to-day variability arises from differences in radiant loading due to cloud cover (Fig. 3); however, at other sites changes in synoptic conditions (e.g., at Sacramento the passage of a cold front) result in quite different energy balance partitioning on consecutive days (Grimmond et al. 1993). Even on cloud-free days, when the diurnal pattern of net all-wave radiation is smooth, and wind direction gives relatively constant and uniform fetch for several hours, hourly ''spikes'' (i.e., unusually high or low values for a single hour) in the convective fluxes are common. Often both Q_E and Q_H rise or fall together, and this is evident for all the 15-min runs that make up the data for an hour. Since the storage heat flux is calculated as a residual, if the diurnal trend in Q^* is smooth and both convective fluxes spike in the same direction, ΔQ_S also will spike, but in the opposite direction. Such spikes also occur on cloudy days when they are often, although not always, associated with changing cloudiness. For any given hour, the convective fluxes are just as likely to spike up as down, hence the long-term ensemble time series of Q_H and Q_E (and thus ΔQ_S) can be fairly smooth (see plots for four of the cities in Grimmond and Oke 1995).

There appears to be no systematic diurnal pattern to this type of variability. In some of the cities, notably A93, A94, Sg94, the greatest variability, both in absolute and relative terms, is in the late morning/middle of day, that is, coincident with the highest storage heat flux. However, elsewhere, for example, Vs92, S91, and C95 variability is evident throughout the day. This hour-to-hour variability is not evident in soil temperatures or soil heat fluxes observed concurrently at the urban sites, although the day-to-day variability is (see data for Sacramento in Grimmond et al. 1993). Therefore, we recommend that individual hourly values of storage heat flux be interpreted with caution and that longer averages (minimum of two hours) are used when considering intradaily data. This recommendation is also supported by the fact that 2 h is the appropriate averaging period according to Wyngaard (1973) in order to measure Q_H to an accuracy of 10% under unstable conditions, at 30 m, with wind speeds of 5 m s^{-1}.

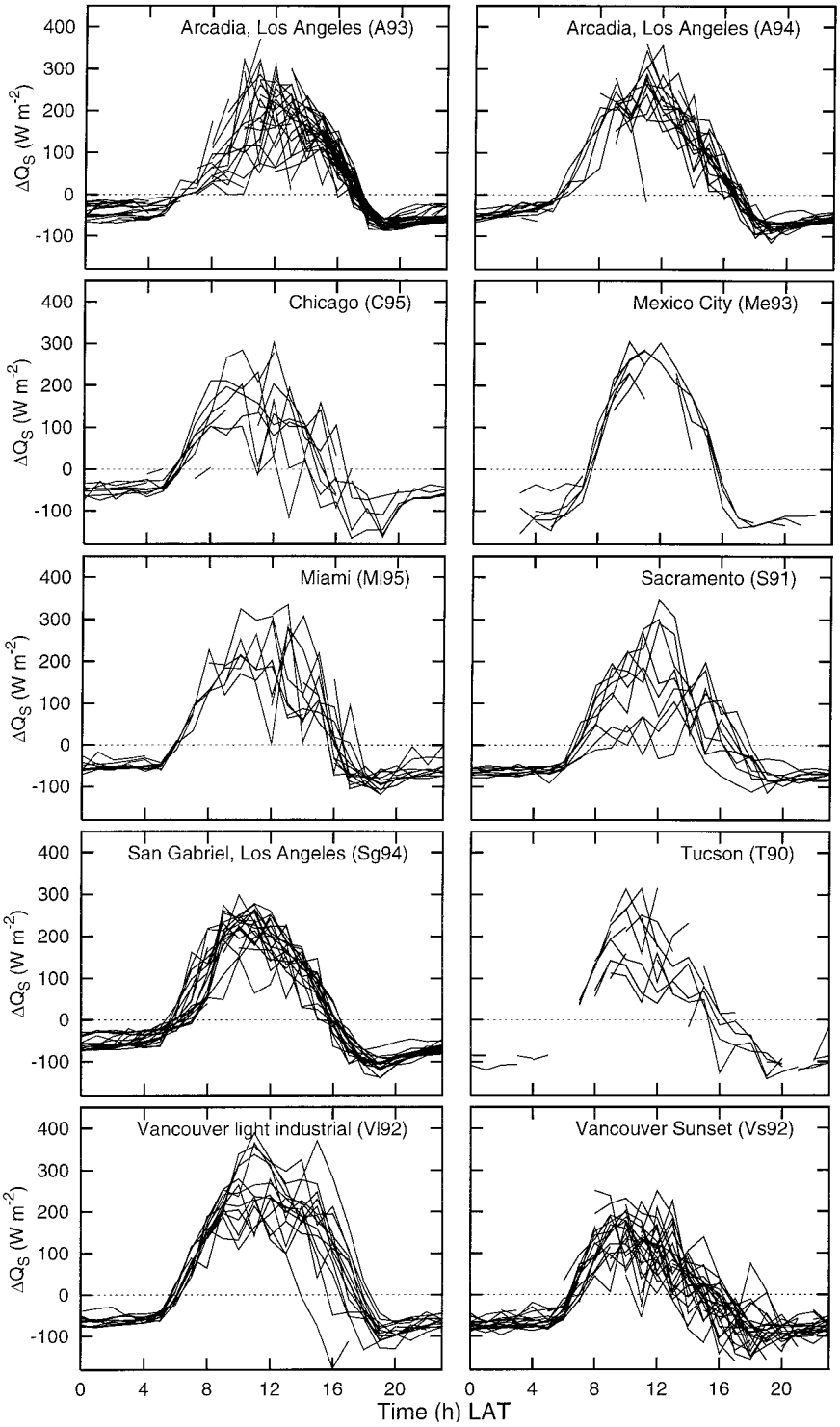

FIG. 2. Hourly storage heat flux (W m^{-2}) for each day of measurements at each site. Data are plotted only for wind directions with reasonably homogeneous fetch (Table 1).

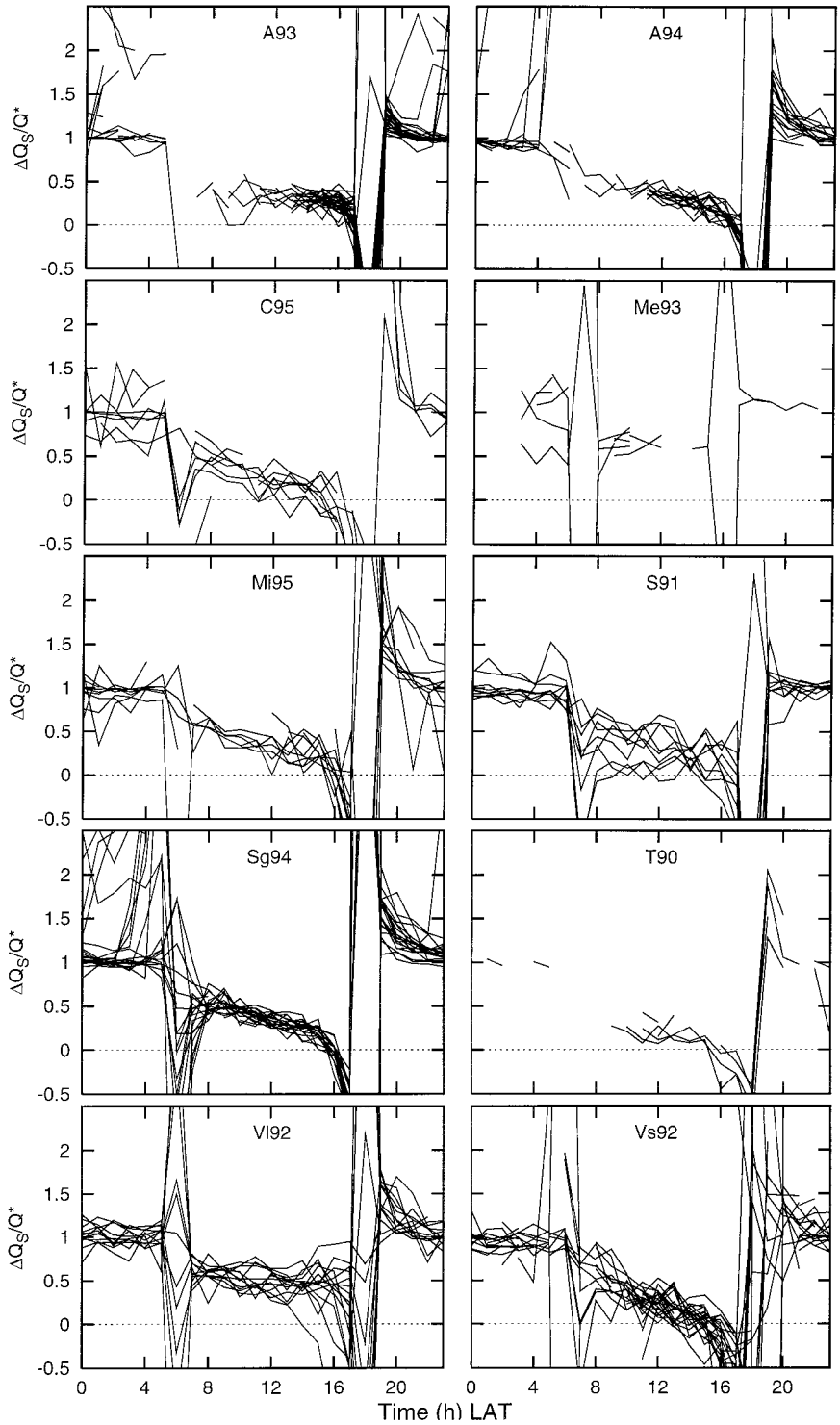

FIG. 3. Hourly $\Delta Q_S/Q^*$ for each day at each site (same hours as Fig. 2).

For the first third of the night ($Q^* < 0$) most of the sites release large amounts of stored heat. This is especially the case for Mexico City and Tucson, where clear, dry conditions are conducive to radiant cooling. This heat release is responsible for the maintenance of positive Q_H for several hours after Q^* becomes an energetic drain (Oke 1988). Beneath roof level in the urban canopy layer this release is slowed by the effect of ho-

TABLE 3. Evaluation of fitted hysteresis model for each site. Coefficients a_1, a_2, and a_3 determined from fitting Eq. (3) to the mean diurnal data for all-sky conditions for each city (see Table 1 for city codes). Statistics derived from correlating Eq. (3) with the fitted coefficients to the hourly data (for the number of hours of data used in the analysis, see Table 1). Cities ordered as in Table 1 (decreasing area built). r^2 is the coefficient of determination, rmse is the root-mean-square-error (W m^{-2}), rmse_{SY} systematic error (W m^{-2}), and rmse_{USY} unsystematic error (W m^{-2}).

Type	a_1	a_2	a_3	Slope	Intercept	r^2	rmse	rmse_{SY}	rmse_{USY}
Me93	0.740	0.069	−37.3	0.996	0.093	0.973	25.2	0.6	25.2
Vl92	0.568	0.217	−29.2	0.933	4.152	0.885	46.6	9.1	45.7
C95	0.288	0.664	−43.5	0.969	34.170	0.606	86.5	33.8	79.6
T90	0.385	0.440	−57.2	0.930	7.246	0.770	65.2	9.9	64.4
Mi95	0.409	0.428	−36.6	0.971	1.824	.0797	55.6	3.6	55.5
Sg94	0.434	0.514	−43.7	1.077	−1.676	0.908	39.9	8.8	38.9
Vs92	0.350	0.656	−48.6	0.982	3.564	0.715	55.4	4.2	55.3
S91	0.385	0.256	−39.2	0.803	0.394	0.730	51.9	19.5	48.2
A94	0.397	0.405	−32.5	1.068	1.153	0.903	41.5	8.5	40.6
A93	0.383	0.161	−28.2	0.974	1.908	0.911	31.8	2.9	31.6

rizon screening on Q^*. This interplay between storage and radiation underlies heat island growth at the microscale. For the rest of the night there is a balance between the storage source and the radiative drain; Λ at all sites lies within the remarkably small range $0.95 < Q^* < 1.05$. Even the very large release from central Mexico City (Fig. 3a) falls within the range because of the large Q^* at its elevation. In Tucson, where most irrigation occurs automatically at night, this release of heat helps sustain positive Q_E fluxes through the night.

In all of the cities there is a distinct hysteresis pattern between the radiative forcing and storage change. This is responsible for the downward slope of Λ during daytime (Fig. 1b) and the loop formed when ΔQ_S is plotted against Q^* (Fig. 1c). In general, the peak in ΔQ_S precedes that of Q^* by 1–2 h. The phase shift is most marked at Vs92 and C95 (the two sites where daytime ΔQ_S is least important), and is least at A93 and Me93. There is no apparent direct connection between the timing of the peak and any single land cover descriptor or meteorological condition (such as onset of the diurnal wind cycle). At all sites the share of the sensible heat going to warm the air rather than the urban fabric increases over the course of the day (Fig. 1d). In the morning hours, the atmosphere is still relatively stable, hence sensible heat flux is transferred more readily into the soil. In the afternoon when the atmosphere is unstable, and the coupling of the surface–atmosphere greatest, the turbulent heat transfer into the atmosphere is more efficient. It might be expected that in the urban areas with greater surface roughness, greater instability, and/or greater wind speeds, that the thermal admittance of the atmosphere relative to the surface ($\mu_A : \mu_S$), and thus Q_H relative to ΔQ_S, would be enhanced. The quantity Q_H is most significant and hysteresis in ΔQ_S is best defined at Vs92, T90, and C95. Although these sites are among the windiest, and Vs92 and C95 are amongst the ''roughest,'' there is no simple relation between $Q_H/\Delta Q_S$ and wind speed. When stratified by hourly wind speed (greater than or less than 5 m s^{-1}), the overall relation between Q_H and ΔQ_S remains the same. Unfortunately, even with the dataset here, insufficient data have been collected for days with sustained high wind speeds to investigate differences from day to day.

The observed phase-lag between Q^* and ΔQ_S seen here is similar to that reported previously in Vancouver (Oke and Cleugh 1987; Grimmond et al. 1991; Roth and Oke 1994). Drawing on the work of Camuffo and Bernardi (1982), Oke and Cleugh (1987) used a hysteresis-type equation to characterize the storage heat flux as

$$\Delta Q_s = a_1 Q^* + a_2 \frac{\partial Q^*}{\partial t} + a_3, \tag{3}$$

in which t is time. The parameter a_1 indicates the overall strength of the dependence of the storage heat flux on net radiation. The parameter a_2 describes the degree and direction of the phase relations between ΔQ_S and Q^*. When a_2 is positive, ΔQ_S precedes the peak in Q^*; when it is zero, the two curves are exactly in phase, that is, there is no hysteresis. The parameter a_3 is an intercept term that indicates the relative timing when ΔQ_S and Q^* turn negative. A large a_3 coefficient indicates ΔQ_S becomes negative much earlier than Q^*; it is the size of ΔQ_S when Q^* becomes negative.

To assess the appropriateness of the form of Eq. (3) for cities other than Vancouver, the coefficients a_1, a_2, and a_3 were fitted statistically to each of the datasets in this study using hourly averaged data. The derivative of net radiation (W m^{-2} h^{-1}) is approximated as

$$\frac{\partial Q^*}{\partial t} = 0.5[Q^*_{t+1} - Q^*_{t-1}]. \tag{4}$$

The data used are the ensemble set ($n = 24$) for all-sky conditions. For an hour to be included in the ensemble average, data for all four 15-min periods had to originate from the acceptable wind directions for that site (Table 1). Table 3 is a statistical evaluation of the goodness of fit of the hysteresis approach for each city.

The hysteresis form performs very well in Los Angeles (A93, A94, and Sg94) and Mexico City (rmse $<$ 42 W m^{-2}), but less well in Chicago, Vancouver, Miami, Sacramento, and Tucson (with rmse up to 87 W m^{-2}). The fitted a_1, a_2, and a_3 coefficients of the hysteresis

model vary significantly between sites. The a_1 parameter is greatest for the Mexico City and Vancouver light industrial sites, and lowest for the Chicago and Vancouver suburban sites. This pattern is expected given the greater importance of the storage heat flux at the downtown and light industrial sites (Table 2). The rank order of a_1 by city approximates the sequence of Λ (Table 2), although at all sites the a_1 coefficients are larger than Λ.

The a_2 parameter is positive at all sites, indicating the peak in ΔQ_S precedes that in Q^* (i.e., the loop is clockwise). The magnitude of the hysteresis loop is greatest at Vs92 and C95, which as noted above were the sites with the earliest peak in ΔQ_S (i.e., greatest phase-shift between Q^* and ΔQ_S) and the lowest daytime Λ. The hysteresis loops are weakest in Me93 and A93. There is no clear relation between land use and a_2, although the coefficients for the urban and light industrial sites are at the lower end of the range (0.07 and 0.22, respectively). Fuchs and Hadas (1972) suggest that hysteresis effects increase in a soil as surface moisture decreases (through an indirect effect on Q_E). The two suburban sites with the greatest hysteresis (highest a_2) are Vs92 from a very dry period during an irrigation ban and C95 data from a very warm period with high evaporation rates. Stratification of the Vs92 data into periods before, during, and after the irrigation ban give a_2 coefficients of 0.59, 0.72, and 0.55, respectively. This further suggests that hysteresis may increase at a site as conditions dry out. However, surface moisture per se cannot explain differences between sites. Rather the interplay of surface roughness, the diurnal wind regime, and surface moisture, in combination, exert an effect.

Interestingly, the a_2 coefficient is quite different for the 2 yr of observations at Arcadia: 0.16 in A93 compared to 0.38 (well-developed hysteresis) in A94. This is notable because both site characteristics and average flux partitioning were similar in the 2 yr (Table 1). Evaporation was greater in 1993, particularly in the early morning (Grimmond and Oke 1999b), while sensible heat fluxes remained constant, resulting in lower ΔQ_S in the morning (i.e., the reduced hysteresis). Analyses reveal this is not attributable to differences in cloud cover between the 2 yr.

The fitted a_3 coefficients vary from -57.2 W m^{-2} at T90 to -28 W m^{-2} at A93. In Tucson the high value, indicating that storage turns negative well before Q^* (see Fig. 1), seems to be associated with enhanced evaporation in mid/late afternoon. The smaller a_3 value at A93 again indicates weak hysteresis at this site, that is, more energy going into storage in the afternoon than at other sites.

There are no simple correlations between the a_1, a_2, and a_3 coefficients and individual surface cover fractions. At a general level, a_1 increases with the area of impervious and roof surfaces, and decreases with the area vegetated. No simple relations are evident for a_2 and a_3. Given the variability of the hysteresis model coefficients from city to city, no generic form of the fitted model can be recommended for use in all urban areas.

6. Other forms of storage heat flux model

Other forms of equation have been proposed to describe the diurnal pattern of storage heat flux for urban areas; for example, linear models (Oke et al. 1981) and hyperbolic functions (Doll et al. 1985). We now know that linear forms are not appropriate for urban areas given the strength of the hysteresis behavior (Fig. 1). Doll et al. (1985) use a *cotangent* function, which does pick up the diurnal hysteresis pattern evident in Λ, but it does not cope well with the nocturnal to daytime transition, nor the nocturnal form of Λ. Doll et al. (1985) also propose a *secant* function, which follows the temporal discontinuities between day and night well, but the daytime form of Λ is flat, hence the hysteresis pattern is not incorporated. Given this, and the results in the preceding section, we conclude that the hysteresis equation is an appropriate form for simulating the storage heat flux in urban areas. However, the goodness of fit varies from city to city, and there are important features, most notably in C95, T90, and S91 that it does not capture (Table 3; Fig. 3).

7. The objective hysteresis model (OHM)

a. Application of OHM

Grimmond et al. (1991) proposed the OHM, which incorporates both the hysteresis nature of the storage heat flux and the surface properties of the site. The steps to apply the OHM at any site are: i) conduct a survey of the area to create an inventory of building dimensions and areal coverage of different surface types; ii) compile a list of the a_1, a_2, and a_3 coefficients for the different surface types (vegetated, paved, roofs, and walls of canyons, water) present in the area; iii) calculate site specific coefficients for the OHM model by weighting those for the individual surface types according to the proportion of the total area occupied by the respective surface types; and iv) estimate ΔQ_S from measured net radiation by summing the contributions by each surface type over all types,

$$\Delta Q_s = \sum_{i=1}^{n} \left[a_{1i} Q^* + a_{2i} \frac{\partial Q^*}{\partial t} + a_{3i} \right]. \qquad (5)$$

The index i identifies a surface type, of which there are n in total. Cautionary comments need to be made when applying this approach at the local scale. There is an error inherent in assuming an areal Q^* (as measured in this study) instead of the individual surface values used in the derivation of the equation for each surface. Bias may be introduced if the area under consideration is made up of surfaces with contrasting radiative exchanges.

TABLE 4. Coefficients for urban surface types used to determine parameters for the OHM.

Surface cover type	Source	OHM coefficients		
		a_1	a_2 (h)	a_3 (W m^{-2})
1. Greenspace/Open				
Mixed forest*	McCaughey (1985)	0.11	0.11	−12.3
Short grass	Doll et al. (1985)	0.32	0.54	−27.4
Bare soil	Novak (1981)	0.38	0.56	−27.3
Bare soil—wet*,**	Fuchs and Hadas (1972)	0.33	0.07	−34.9
Bare soil—dry*	Fuchs and Hadas (1972)	0.35	0.43	−36.5
Soil*	Asaeada and Ca (1993)	0.36	0.27	−42.4
Water—shallow turbid*	Souch et al. (1998)	0.50	0.21	−39.1
2. Rooftop				
Vancouver	Yap (1973)	0.17	0.10	−17
Uppsala**	Taesler (1980)	0.44	0.57	−28.9
Kyoto*	Yoshida et al. (1990–91)	0.82	0.34	−55.7
3. Paved/Impervious				
Concrete	Doll et al. (1985)	0.81	0.48	−79.9
Concrete*	Asaeada and Ca (1993)	0.85	0.32	−28.5
Asphalt	Narita et al. (1984)	0.36	0.23	−19.3
Asphalt*	Asaeada and Ca (1993)	0.64	0.32	−43.6
Asphalt*	Anandakumar (1998)	0.82	0.68	−20.1
4. Canyon				
N–S canyon	Nunez (1974)	0.32	0.01	−27.7
E–W canyon*	Yoshida et al. (1990–91)	0.71	0.04	−39.7

* ''New'' coefficients, that is, post Grimmond et al. (1991).
** Not used in any runs.

For the sites in this study (Table 1), the model is evaluated using the a_1, a_2, and a_3 coefficients derived from published data for common surface types found in urban environments (Table 4). This list is slightly more extensive than that used by Grimmond et al. (1991). For some surface types, notably bare soil and concrete, more recent sets of coefficients are very similar to those used previously, but for others the new values are quite different. For example, the a_1 coefficients for the rooftop, asphalt, and the E–W canyon, are all higher than previously used (Table 4).

In this study four surface characteristics are used: greenspace/open, rooftop, paved/impervious, and canyon. All coefficients for surfaces within each category are averaged. Within the greenspace category (vegetated/bare soil surfaces) the coefficients are similar, but those for the canyons and rooftops cover a wide range, so there is uncertainty as to which should be used. Clearly more data need to be collected to document the precise nature of the coefficients for these and a fuller array of urban materials. In addition, more observations are needed over a wider range of seasonal/annual conditions. Analysis of annual data collected by Anandakumar (1999) suggest some variability in the magnitude, and even the sign of the coefficients, notably a_3. These effects are not considered here.

b. Evaluation of the OHM

Using the GIS developed for each city and FSAM (as described above), surface characteristics of the source areas for each hour of observations were calculated and used to weight the OHM coefficients. The ΔQ_S is calculated using the measured Q^* and the appropriate a_1, a_2, and a_3 coefficients. In the first part of this analysis the OHM is evaluated only for those hours (all 15-min periods) in each city when measurements were derived from source areas with similar surface characteristics (the directions listed in Table 1). Later we consider the performance for all hours regardless of direction. This provides a broader test of the OHM and provides insight into its ability to pick up differences in ΔQ_S for areas of differing surface cover within a city. Two additional datasets are included here. The first collected in Vancouver in 1989 (Vs89), described by Roth and Oke (1994), at the same site as Vs92. The second collected in Chicago in 1992 (C92), described by Grimmond et al. (1994), at a site close to C95. These sites were not used in part 1 of this paper because insufficient data were collected from uniform fetch to allow a full characterization of the diurnal characteristics of flux partitioning; however, they provide additional observations to test the OHM.

Results of the evaluation of the OHM using hourly data are summarized in Figs. 4, 5, and 6, and Tables 5 and 6. In the ensemble plots (Fig. 4), which are the mean of the hourly computations, three sets of storage heat flux data are plotted:

1) *measured* data [i.e., the residual from the observed energy balance fluxes; Eq. (2)];
2) ΔQ_S modeled using the *fitted* coefficients from the ensemble data for all-sky conditions (Table 3); and

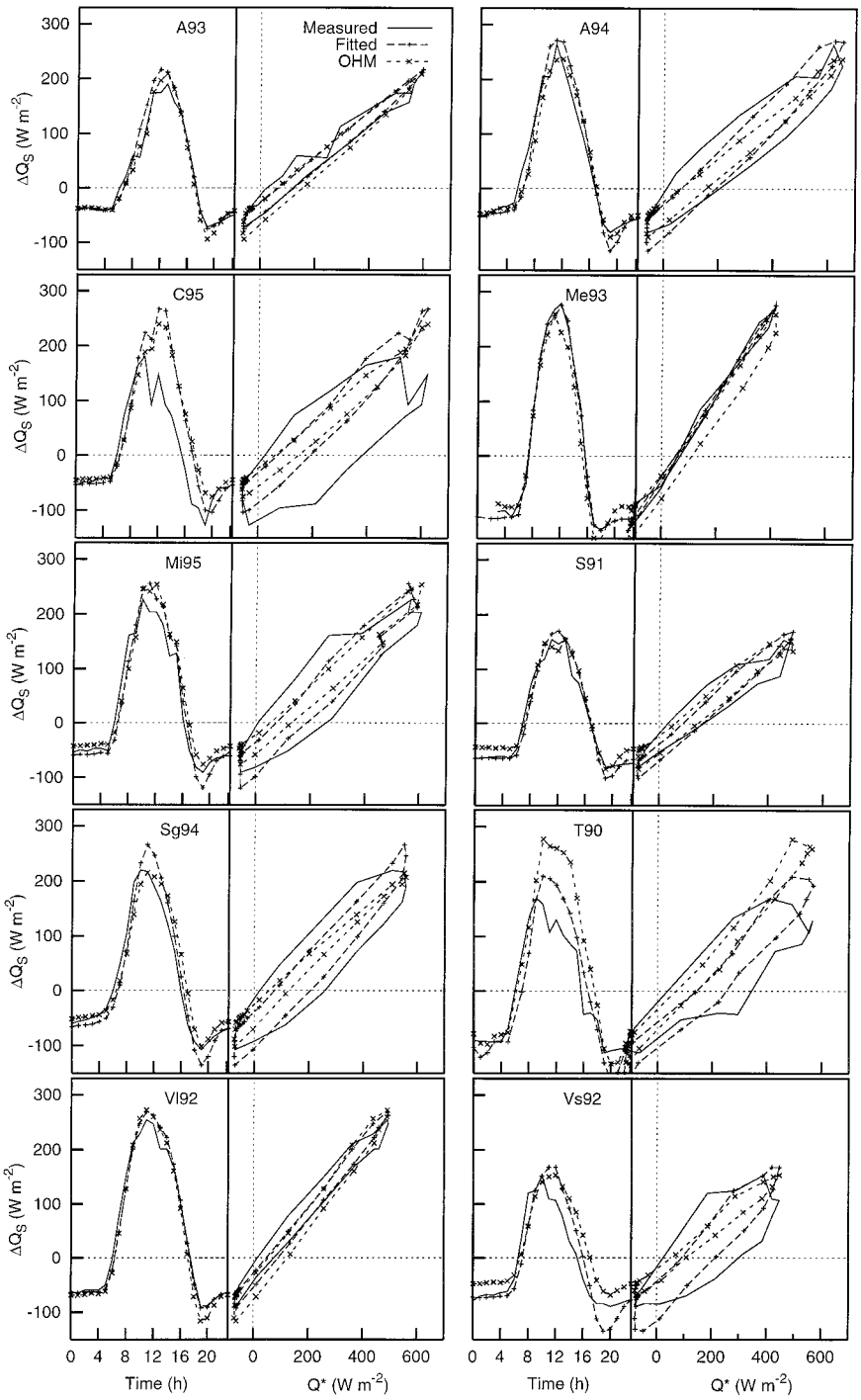

FIG. 4. Mean diurnal measured and modeled (fitted and the OHM) storage heat flux (W m^{-2}) vs time (left side of panel) and hysteresis loops of storage heat flux vs net radiation (right side of panel) for each dataset.

3) ΔQ_S modeled using the OHM.

Figure 5 consists of scatterplots of the hourly measured versus modeled data. The data from the selected wind directions (Table 1) are distinguished from all other hours by different symbols.

c. Performance of the OHM

Before considering the performance of the OHM on a site-by-site basis, we consider the effects of adding/dropping selected surface coefficients and of describing

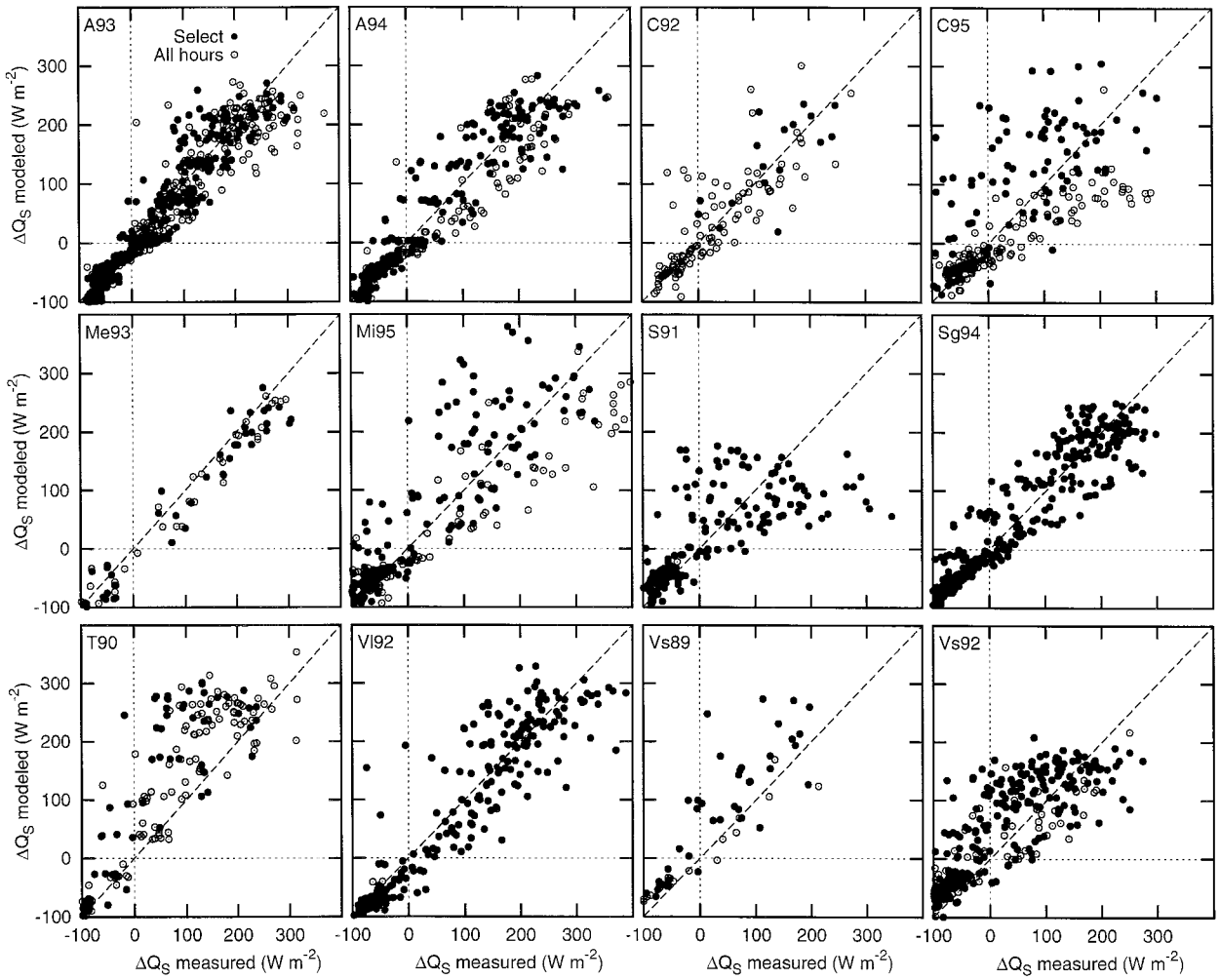

FIG. 5. Scatterplots of hourly measured vs modeled storage heat flux (W m^{-2}) using simplified surface description (A_V, A_I, and A_R) and the coefficients listed in Table 4. Solid circles are hours from selected wind directions (Table 4); open circles all other hours of observation. Statistics of goodness of fit reported in Table 5.

surface cover in different ways upon the performance of the OHM.

Inclusion of the ''new'' coefficients listed in Table 4 significantly improves the performance of the objective hysteresis model over its original form when evaluated using these data. The problems of ''capping'' (the inability of the OHM in its original form to simulate the highest observed ΔQ_S values), reported by Grimmond et al. (1991) and Roth and Oke (1994), has largely disappeared due to the inclusion of the new coefficients (see further discussion below).

The OHM performance is improved slightly (reduction in rmse <5 W m^{-2}) if the area vegetated (A_V) is subdivided into those fractions covered by trees, irrigated grass, open water, and unmanaged cover (bare soil and waste land), and these are used to weight the appropriate coefficients in Table 4. The degree of improvement is greatest for Vs89 and T90, sites where the OHM works least well. The effect at the most heavily vegetated sites (A93, A94, Sg94) is marginal.

The OHM also was evaluated using planimetric (2D) surface cover as the basis for weighting the coefficients (as opposed to including the full three-dimensional area of the walls), and using various schemes to parameterize the fraction of walls sunlit and shaded. The effect of these modifications on the performance of the OHM is marginal (<5 W m^{-2} in rmse) at all sites except C95, Me93, and Vs89/92. At these sites the OHM performs better if the walls/canyon data (the three-dimensional geometry of the sites) are excluded. This is particularly noteworthy because these are the three sites where walls are most important (A_W 43%, 38%, and 30%, respectively). For both Me93 and C95 it is the systematic error that is reduced by removing the walls/canyons. This strongly suggests that the model coefficients for the canyons are poorly specified

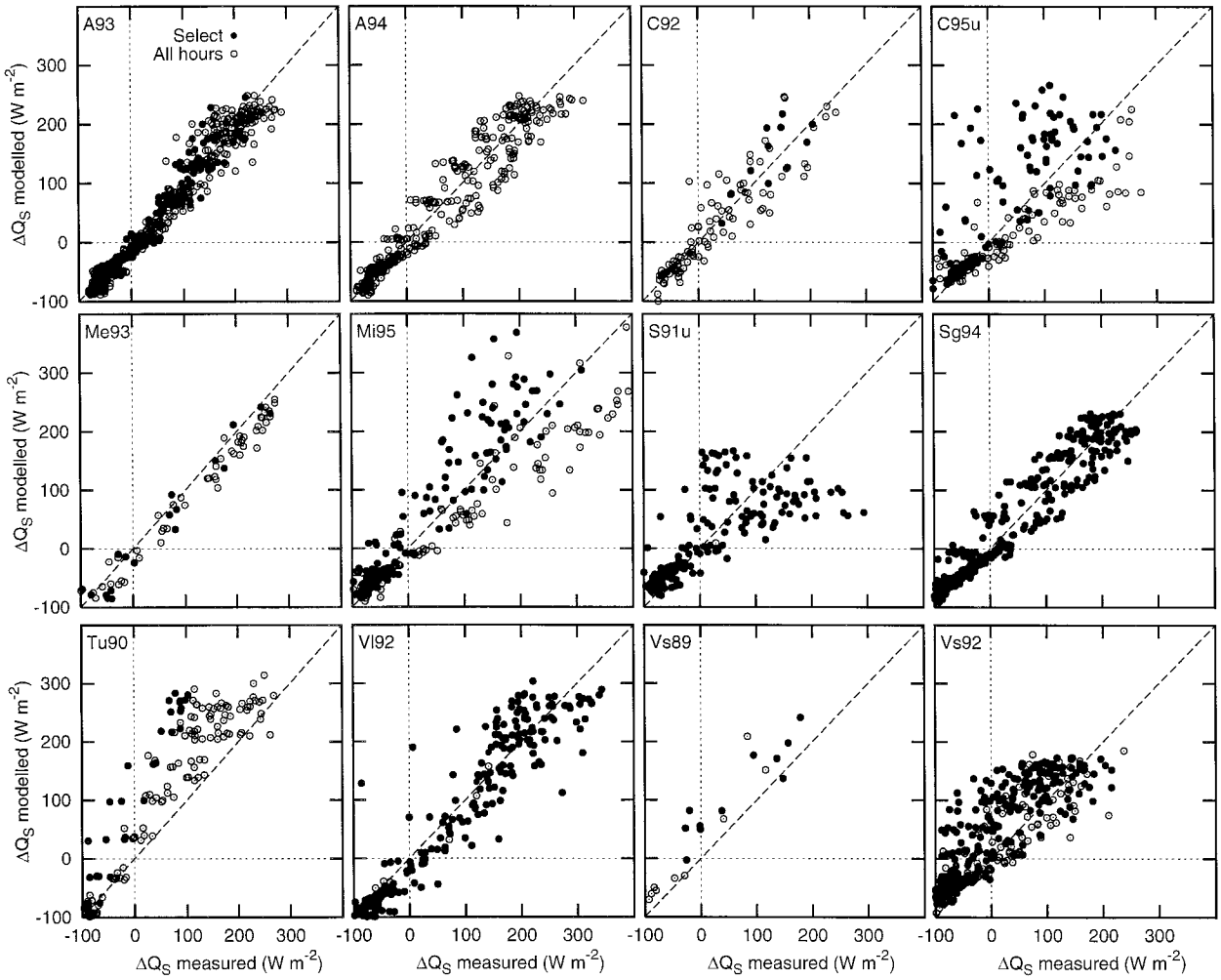

FIG. 6. Scatterplots of two-hourly measured vs modeled storage heat flux (W m^{-2}) (see text for explanation). Solid circles are hours from selected wind directions (Table 4); open circles all other hours of observation. Statistics of goodness of fit reported in Table 6.

TABLE 5. Statistical performance of the OHM at the hourly timescale. Fluxes are determined for hours when all four 15-min periods are from acceptable wind directions. Canyons are not included in the surface description, and all coefficients for the area greenspace/open are averaged equally.

Site	*N*	Slope	Intercept (W m^{-2})	r^2	rmse (W m^{-2})	$rmse_{SY}$ (W m^{-2})	$rmse_{USY}$ (W m^{-2})
A93	424	0.966	−4.0	0.915	29.0	5.7	28.4
A94	290	0.933	5.8	0.900	35.8	8.6	34.7
C95	163	0.806	38.8	0.562	83.3	41.0	72.5
C92	24	0.907	14.5	0.825	45.9	12.3	44.2
Me93	61	0.892	−6.8	0.961	33.6	19.2	27.6
Mi95	204	0.975	22.9	0.788	61.9	22.7	57.5
S91	222	0.548	5.0	0.556	66.0	44.9	48.4
Sg94	467	0.873	9.6	0.898	37.2	16.2	33.4
T90	75	1.206	66.1	0.748	107.4	73.2	78.6
Vl92	312	0.962	−4.5	0.880	48.9	8.3	48.2
Vs89	42	0.967	53.2	0.753	74.7	52.5	53.2
Vs92	464	0.745	30.8	0.674	62.9	40.4	48.2

TABLE 6. Statistical performance for the same conditions as in Table 5 but with hourly fluxes averaged over 2 h.

Site	N	Slope	Intercept (W m^{-2})	r^2	rmse (W m^{-2})	rmse$_{SY}$ (W m^{-2})	rmse$_{USY}$ (W m^{-2})
A93	272	1.002	−6.4	0.956	18.8	6.4	17.7
A94	215	1.021	8.0	0.955	22.6	8.5	21.0
C95	136	0.915	40.5	0.617	76.7	40.4	65.3
C92	17	1.024	9.5	0.918	31.2	11.4	29.1
Me93	28	0.952	−8.5	0.969	22.9	10.0	20.6
Mi95	181	1.108	23.0	0.884	48.8	26.6	41.0
S91	220	0.578	5.1	0.591	59.3	39.1	44.5
Sg94	455	0.899	9.3	0.927	30.1	13.3	26.9
T90	32	1.781	106.4	0.933	125.5	120.3	35.8
Vl92	302	0.992	−6.1	0.910	40.8	6.6	40.3
Vs89	11	0.861	60.0	0.859	59.3	52.6	27.3
Vs92	298	0.843	38.7	0.751	57.9	40.9	41.0

[note there is a factor of 2 difference in the a_1 values for Nunez (1974) and Yoshida et al. (1990–91) reported in Table 4], and/or the walls are incorrectly described. Arnfield and Grimmond (1998) demonstrate with numerical modeling that the OHM-type coefficients change significantly depending on canyon geometry and/or orientation. If the OHM is run just with the Nunez (1974) coefficients performance is better at all sites (notably C95 and Vs89/92 where rmse drops by the order of 25 W m^{-2}) except Me93. However, improvement with no canyons/walls included is limited. Alternatively, if the model is run just with the Yoshida et al. (1990–91) coefficients, performance is better in Me93 (where rmse increases by 24 W m^{-2}), but poorer at all other sites. These findings clearly indicate the need for more data to be collected for canyons of different geometries in different locations. Furthermore, the coefficients presented in Table 4 are derived from studies of ''dry'' canyons, which are not fully representative of the urban sites considered here.

Given that our objective is to develop a simple model of heat storage in urban areas, we conclude that increasing the complexity and/or detail of surface description is not warranted. Incorporating 3D versus 2D surface area, considering trees, grass, open water, etc. separately rather than aggregating them into an area of greenspace/open, does not result in a significant improvement in the OHM performance across all sites. Therefore we recommend using the simplest surface description that considers only the plan area of the impervious surfaces and rooftops, and combines all greenspace, open and bare ground areas into one category (i.e., A_I, A_R, and A_V).

Clearly performance of the OHM is not equally good across all sites. It works best for more urban sites (Me93, Vl92), the sites in Los Angeles (A93, A94, and Sg94), and Chicago (in 1992 but not 1995). Here we focus on where the model works well and poorly, to gain greater insight into the nature of the storage heat flux term in urban areas. First, we consider the average diurnal pattern and then intradaily timescales and hourly and two hourly fluxes.

1) ENSEMBLE DIURNAL PATTERN

In terms of the average diurnal pattern (Fig. 4), the OHM is able to capture well the magnitude of the peak values and of the daily hysteresis in A93, A94, Vl92, and S91. At Me93 it simulates both the peak and the daily pattern well, but systematically underpredicts afternoon values. It overpredicts peak values in T90 and Sg94 (slightly). The OHM is unable to capture the pronounced hysteresis measured at C95 and Vs92; consequently, it overpredicts midday/early afternoon values at these sites.

It is useful to compare the performance of the OHM against the fitted form of the model at each site to gain insight into how well the databases describe the respective sites, and how well the weighting system works in simulating the integrated storage response of the urban system. At A93, A94, C95, Mi95, Sg94, Vl92, and Vs92 the performance of the fitted model and the OHM are effectively the same (differences in rmse are approximately ± 5 W m^{-2}). At most of these sites both the fitted and objective forms of the model perform well, that is, both the model form and surface parameters are appropriately specified. At Mi95 and C95 neither the OHM nor the fitted model perform well. At these sites it is not the specification of the surface parameters, but the general form of the model itself that is the problem. In both instances neither the fitted nor the objective forms capture the magnitude of the hysteresis observed. At all sites where the OHM and the fitted model have a similar level of performance, with the exception of Vl92, vegetation is a significant component of the suburban landscape. As already noted, the coefficients for this surface type are fairly consistent and well defined (Table 4).

At Me93, S90u, and T90, the OHM does less well than the fitted form of the model (rmse$_{SY}$ increases by 20 W m^{-2}, 20 W m^{-2}, and 65 W m^{-2}, respectively, for the OHM, with little change in the rmse$_{USY}$). This suggests either there is a problem with the description of these sites or with the specification of the coefficients for the dominant surface types.

At Me93, where there is effectively no systematic error with the fitted form of the model ($rmse_{SY} < 1$ W m^{-2}), the OHM underpredicts ΔQ_S in the afternoon; it simulates too much hysteresis. Me93 is the site where measured ΔQ_S shows least hysteresis (evident in the fitted a_2 coefficient in Table 3 and Fig. 4). It is notable that this is the site where canyons/walls are most important, and as Table 4 shows these have the lowest hysteresis coefficients. It is also the only site where measurements were conducted in the winter. Anandakumar (1999) suggests the a_3 coefficient (at least for asphalt) becomes positive in winter. This suggests that the OHM hysteresis parameters are incorrectly specified for this site. However, at this stage we cannot resolve whether this is a function of the time of the year or the material properties/geometry of the site. Despite this problem at Me93 the overall performance of the OHM is good.

The difference between the fitted and objective models is most pronounced in Tucson. At this site the fitted form of the model simulates the observed diurnal pattern reasonably well, but the OHM greatly overpredicts ΔQ_S from the peak midday values until late afternoon (Fig. 4). The drop in ΔQ_S late in the afternoon is attributed to an increase in Q_E at this time as people irrigate their gardens and use evaporative (swamp) coolers to maintain tolerable temperatures in many houses (Grimmond and Oke 1999b). Both these activities result in a decrease in heat storage (the intent of the inhabitants). Clearly the OHM in its present form cannot simulate such effects. Tucson, like San Gabriel (where the OHM works reasonably well), has a large portion of the surface covered by impervious materials. The site is dominated by small houses, with xeriscape landscaping, and wide roads. However, it has a very different storage heat flux regime to that of San Gabriel (especially lower measured values in the afternoon). The a_1 coefficient for impervious materials (Table 4) is high; undoubtedly this contributes to the high OHM predictions at this site. Attempts to force the OHM to perform better at T90, by altering the way the surface is described and varying the model coefficients used, did not yield greatly improved results.

In Sacramento the problem with the OHM is different. Figure 2 shows clearly that storage heat fluxes were markedly different on different days. Mid-way through the measurement period a cold front passed through. The net effect was a drop in air temperature, reduction in vapor pressure deficits, and increased wind speeds. Bowen ratios rose as Q_H increased while Q_E remained fairly constant. As a consequence ΔQ_S was much lower after the passage of the cold front. Independent support for this is provided by the soil temperature and soil heat flux observed at the site; values are significantly different for the two periods (Grimmond et al. 1993). The fitted model is actually a fit to the average of these two sets of conditions, hence it has a high systematic error (Table 5). The OHM is unable to capture this synoptic-scale effect (and changes in wind speeds, vapor deficits, and air temperatures), consequently it too does a poor job of simulating ΔQ_S. This synoptic-scale effect on the surface flux partitioning is more evident at this site than any other, and day-to-day variability that is not radiatively driven is also less evident elsewhere (Fig. 3).

The OHM was evaluated separately for clear and cloudy days, to identify how well the model deals with changing radiation conditions, and to ensure the errors under discussion are not a result of variable cloud and radiation conditions influencing the measurements. Overall the OHM performs slightly better under clear-sky conditions (systematic errors increase under cloudy conditions), with the exceptions of Sg94 and Mi95 (where improvement in the OHM under cloudy conditions results from a reduction in unsystematic errors). However, in most cases the number of clear versus cloudy data points for each site are quite unequal, thus any differences should be interpreted with caution.

2) HOURLY FLUXES

In terms of hourly fluxes (Fig. 5; Table 5) the OHM does a very good job ($r^2 > 0.9$) at A93, A94, Me93, and a good job ($r^2 > 0.8$) at C92, Sg94, Vl92 (although there are distinct outliers). Performance is poor for T90 (for the reasons already described above) and mixed (i.e., it works for some hours, but not others) for C95, Mi95, Vs89, and Vs92. The general pattern at most of the sites is that hourly values are underpredicted in the morning, and overpredicted in the afternoon. As already noted, the OHM cannot capture the marked hysteresis evident at some of the suburban sites (notably C95, Mi95, and Vs92). Interestingly, in Vancouver, although the OHM performs similarly for 1989 and 1992, the performance was better in Vs89 suggesting some effect of the extremely dry conditions in 1992. However, problems do exist in 1989 too, suggesting at the Vs site errors with the OHM cannot be attributed to the drought conditions of 1992 alone; rather they must be due also to other characteristics of the site that the OHM cannot capture.

When hour-to-hour variability in ΔQ_S is caused by changes in radiative conditions (i.e., cloud cover), the OHM simulates this appropriately. However, it cannot model the hour-to-hour variability due to the spiking up or down of the convective fluxes under uniform radiative and wind (i.e., fetch) conditions. In order to determine the effect of this on the performance of the OHM, the model also was evaluated over 2-h periods. To do this the OHM is run at the hourly time step and the results averaged over 2 h (see earlier comments about averaging periods). Many of the observed ΔQ_S spikes (which are commonly only of 1-h duration) are filtered out. Consequently, performance of the model is improved for all sites (rmse drops by 6–16 W m^{-2}) except Tucson, where systematic errors become more obvious (Fig. 6; Table 6). Greatest improvements are

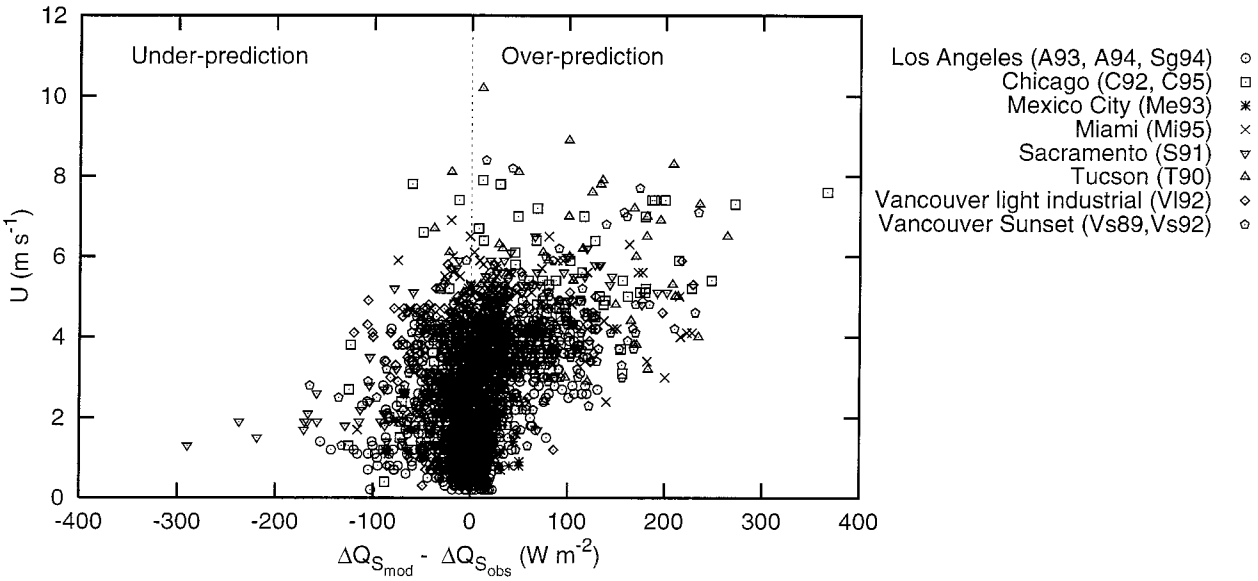

FIG. 7. Hourly OHM errors (predicted–observed) vs wind speed. Each city is distinguished by different symbols.

for A93, A94, C92, Me93, Mi95, and Vs89; rmse is reduced by >10 W m^{-2}. As expected, most of the benefit comes from a reduction in the unsystematic error (Table 6). If the OHM is run at a 3-h time step, model performance is slightly better again (rmse reduced by up to a further 5 W m^{-2}). Therefore, depending on the application, the timescale of interest, and the error tolerance, averaging over 2- or 3-h periods may be a more appropriate way to employ the OHM for applications at subdaily timescales.

However, even when averaged over a 2-h period there are errors with the OHM, particularly at C95, S91, and T90. Sacramento and Tucson have already been discussed and reasons why the OHM did not work during those measurement periods have been outlined. As we have noted, the OHM by design is a very simple radiatively driven model (based on a simple surface parameterization). Clearly other factors affect heat partitioning between the surface, the substrate and the atmosphere, notably roughness and wind speed. Here we consider the effects of wind (peak values and diurnal patterns) at each of the sites. In general, for the sites where the OHM performs best (A93, A94, Sg94, Me93), wind speeds remain below 2 m s^{-1} until midmorning, peak in the midafternoon at approximately 4 m s^{-1}, and are very similar from day to day (see data presented in Grimmond and Oke 1995; Grimmond et al. 1996). The sites where the OHM performs least well (notably C95, S90, T90, Mi95, and Vs92) are the windiest: winds pick up earlier in the morning (>2 m s^{-1} by 0800), drop off more slowly in the afternoon, and peak at higher values (Fig. 7) (up to 7 m s^{-1} on average in T90). Furthermore at these sites the wind regime is more variable on a day-to-day basis.

When the OHM errors are plotted against wind speed (Fig. 7), it is evident that the greatest overpredictions are associated with higher wind speeds (notably in C95, T90, and Vs92), and the greatest underpredictions (of which there are very few, notably only in S91) with lowest wind speeds. However, it is important to note that at both high and low wind speeds the OHM does make accurate predictions. It is notable that it works very well at Vl92, a site with a wind regime more similar to the poorer modeled sites. Also in Mi95, a site that experienced high wind speeds, for some of these hours the OHM did well, for others it did not. Wind is only one of several factors influencing the portion of the available energy going into storage and therefore the performance of the OHM, which only accounts for radiation.

In C95, the OHM does do better on days when it is cooler, with lower wind speeds, and in more neutral stability conditions. On these days flux partitioning (notably Q_E) was more like that observed at the other suburban sites (Table 2). As already noted, under the very hot conditions in Chicago in 1995, residents extensively watered their gardens, the combination of plentiful external water and high wind speeds early in the morning resulted in large latent heat flux and lower than expected values of ΔQ_S. For Vs92 the higher wind speeds, in a period with very little external water, resulted in enhanced sensible heat flux. Thus depending on surface conditions (plentiful or limited water) the OHM may yield errors as a consequence of enhancement of either of the convective fluxes. When the OHM is used, attention should be directed to the diurnal wind regime and surface moisture status of the site under investigation to assess likely effects and potential sources of error.

On an hourly basis, and at all sites, the OHM does a

reasonable job at night. It simulates well the magnitude of the nocturnal flux, its trend, and the transition times in the morning and late afternoon from negative to positive heat flux and vice versa (Figs. 4 and 5). When interpreting nighttime fluxes it is important to realize that measurement errors for the convective fluxes are likely to be larger proportionally; thus there is greater uncertainty in measured ΔQ_S.

The OHM also was evaluated for all hours when data were collected at each of the sites regardless of wind direction, constancy of direction within each hour, or fetch characteristics (additional points are plotted as open circles on Figs. 5 and 6). This represents a much broader test of the OHM. At all sites, except the three where all wind directions were already analyzed (Table 1), this results in at least a doubling of the number of hours under consideration. In Chicago (1995), Arcadia and Miami fluxes representative of large areas of greenspace then become included. In general, the performance of the OHM remains the same (change in rmse <5 W m^{-2}) at the sites where it performs well. Performance decreases in Mi95 (rmse $<$ 10 W m^{-2}), but improves in C95, T90, Vs89, and Vs92 (in part a statistical artifact of the increased number of data points). Overall this shows the OHM is fairly robust and is capable of handling differences in ΔQ_S for different surface types within a city.

8. Conclusions

The storage heat flux, determined as the residual of energy balance observations, is a significant component of the energy balance at all of the urban sites studied. It accounts for 17%–58% of the daytime net radiation. When normalized by net all-wave radiation, storage heat flux is greater at the more urban (downtown and light industrial) sites. Considered at the hourly timescale ΔQ_S is variable. This results from real hour-to-hour variability in the convective fluxes, even under conditions of steady radiative forcing and uniform fetch. As a result we recommend that if the diurnal variation of ΔQ_S is of interest, two-hourly averages (at a minimum) are more appropriate. There is a distinct phase-lag in the relationship between ΔQ_S and Q^* in each city. It is demonstrated that a hysteresis form equation provides an appropriate way to model the flux.

The objective hysteresis model of Grimmond et al. (1991) provides an objective means of modeling storage heat flux patterns of a complex system. The OHM is evaluated for each of 10 sites/times in seven cities using observations of net radiation and an expanded set of statistical coefficients. Given its simplicity, its performance is remarkably good particularly in the more urban (downtown) and light industrial sites and in residential neighborhoods with fairly extensive, irrigated greenspace, with fairly low wind speeds (especially in the morning). For hourly values the rmse ranges from 30–80 W m^{-2} (except for Tucson). The OHM simulates the mean diurnal pattern well, although at some sites it tends to overestimate ΔQ_S particularly in the afternoon. There are important features that the model does not capture, notably the strength of the daily hysteresis evident at some of the suburban sites. Problems also arise because of the hour-to-hour and day-to-day variability in the convective fluxes, which may be attributed in part to surface moisture, wind speed, and synoptic conditions at each of the sites. To improve the OHM further, the conductive and convective fluxes need to be parameterized simultaneously and the effects of wind speed and moisture (in terms of extremes of wetness and dryness) incorporated. At this stage averaging results over 2 h may be a more appropriate way to employ the OHM for applications at less than the daily timescale. However, despite these limitations the OHM provides a good approximation of heat storage in urban areas, although caution should be used in windy environments. It is likely to provide appropriate storage heat fluxes as part of the surface boundary conditions for local to mesoscale meteorological models of airflow (e.g., Taha 1999). Further refinement of the OHM will lie with the incorporation of wind and surface wetness related effects.

The performance of the OHM has been improved significantly with the addition of new coefficients derived from published data. However, one of the major limitations to the application of the OHM remains the sparse data to represent the relation between ΔQ_S and Q^* for individual surface types. The data for the vegetated/bare soil surfaces are very similar, but the coefficients for the canyons and roof tops cover a wide range. This points to the need for more work on the storage characteristics of these components of the urban fabric.

Acknowledgments. We would like to thank the many colleagues and field assistants who have participated in these measurement campaigns, and the organizations and individuals who made the sites available. In particular we would like to thank: Drs. Ernesto Jauregui (UNAM, Mexico), Rachel Spronken Smith (Canterbury, New Zealand), Catherine Souch (IUPUI, United States), Hans Peter Schmid (IU, United States) Jamie Voogt (Western Ontario, Canada), Helen Cleugh (CSIRO, Australia), Matthias Roth (UBC, Canada), Gordon Heisler and Dave Nowak (USFS Syracuse, United States), Greg McPherson and Jim Simpson (USFS Davis, United States), Richard Grant (Purdue, United States), and Mark Demanes, Mark Hubble and Tom King (IU, United States), and Trevor Newton (UBC, Canada) for their many contributions. This research has been funded by the USDA Forest Service (Grimmond), Southern California Edison (Grimmond), Indiana University (Grimmond), Natural Sciences and Engineering Research Council of Canada (Oke), and the Atmospheric Environment Service of Environment Canada (Oke).

REFERENCES

Anandakumar, K., 1999: A study of the partition of net radiation into heat fluxes on a dry asphalt surface. *Atmos. Environ.*, in press.

Arnfield, J., and C. S. B. Grimmond, 1998: An urban canyon energy budget model and its application to urban storage heat flux modelling. *Energy Build.,* **27,** 61–68.

Asaeda, T., and V. T. Ca, 1993: The subsurface transport of heat and moisture and its effect on the environment: A numerical model. *Bound.-Layer Meteor.,* **65,** 159–179.

Camuffo, D., and A. Bernardi, 1982: An observational study of heat fluxes and the relationship with net radiation. *Bound.-Layer Meteor.,* **23,** 359–368.

Doll, D., J. K. S. Ching, and J. Kaneshiro, 1985: Parameterisation of subsurface heating for soil and concrete using net radiation data. *Bound.-Layer Meteor.,* **32,** 351–372.

Ellefsen, R., 1985: Urban terrain zone characteristics. *Tech. Monogr.,* No. 18-87, U.S. Army Engineering Laboratory, Aberdeen Proving Ground, MD, 350 pp.

Fuchs, M., and A. Hadas, 1972: The heat flux density in a non-homogeneous bare loessial soil. *Bound.-Layer Meteor.,* **3,** 191–200.

Grimmond, C. S. B., 1992: The suburban energy balance: Methodological considerations and results for a mid-latitude west coast city under winter and spring conditions. *Int. J. Climatol.,* **12,** 481–497.

——, 1996: Dynamically determined parameters for urban energy and water exchange modelling. *GIS and Environmental Modeling: Progress and Research Issues,* M. F. Goodchild et al., Eds., GIS World Books, 305–309.

——, and T. R. Oke, 1995: Comparison of heat fluxes from summertime observations in the suburbs of four North American cities. *J. Appl. Meteor.,* **34,** 873–889.

——, and ——, 1999a: Aerodynamic properties of urban areas derived from analysis of surface form. *J. Appl. Meteor.* in press.

——, and ——, 1999b: Variability of urban evaporation rates with land use. *IAHS Publ.,* **259,** 235–243.

——, and C. Souch, 1994: Surface description for urban climate studies: A GIS based methodology. *Geocarto Int.,* **9,** 47–59.

——, H. A. Cleugh, and T. R. Oke, 1991: An objective urban heat storage model and its comparison with other schemes. *Atmos. Environ.,* **25B,** 311–326.

——, T. R. Oke, and H. A. Cleugh, 1993: The role of ''rural'' in comparisons of observed suburban—rural flux differences. Exchange processes at the land surface for a range of space and time scales. *IAHS Publ.,* **212,** 165–174.

——, C. Souch, R. H. Grant, and G. Heisler, 1994: Local scale energy and water exchanges in a Chicago neighborhood. Chicago's Urban Forest Ecosystem: Results of the Chicago Urban Forest Climate Project. USDA Forest Service Northeastern Forest Experiment Station, General Tech. Rep. NE-186, 41–61. [Available from Northeastern Forest Experiment Station, 5 Radnor Corporate Center, 100 Matsouford Rd., Suite 200, P.O. Box 6775, Radnor, PA 19087-4585.]

——, ——, and M. Hubble, 1996: The influence of tree cover on summertime surface energy balance fluxes, San Gabriel Valley, Los Angeles. *Climate Res.,* **6,** 45–57.

King, T. S., and C. S. B. Grimmond, 1997: Transfer mechanisms over an urban surface for water vapor, sensible heat and momentum. Preprints, *12th Conf. on Boundary Layers and Turbulence,* Vancouver, BC, Canada, Amer. Meteor. Soc., 455–456.

McCaughey, J., 1985: Energy balance storage terms in a mature mixed forest at Petawawa Ontario—A case study. *Bound.-Layer Meteor.,* **31,** 89–101.

Narita, K., T. Sekine, and T. Tokuoka, 1984: Thermal properties of urban surface materials—Study on heat balance at asphalt pavement. *Geogr. Rev. Japan,* **57**(A), 639–651.

NOAA, 1995: Chicago IL (ORD) Local Climatological Data Monthly Summary. National Oceanic and Atmospheric Administration, 4 pp.

Novak, M. D., 1981: The moisture and thermal regimes of a bare soil in the Lower Fraser Valley during spring. Ph.D. thesis, The University of British Columbia, Vancouver, BC, Canada, 153 pp.

Nunez, M., 1974: The energy balance of an urban canyon. Ph.D. Thesis, The University of British Columbia, Vancouver, 161 pp.

Oke, T. R., 1987: *Boundary Layer Climates.* Routledge, 435 pp.

——, 1988: The urban energy balance. *Prog. Phys. Geogr.,* **12,** 471–508.

——, and H. A. Cleugh, 1987: Urban heat storage derived as energy budget residuals. *Bound.-Layer Meteor.,* **39,** 233–245.

——, B. D. Kalanda, and D. G. Steyn, 1981: Parameterisation of heat storage in urban areas. *Urban Ecol.,* **5,** 45–54.

——, H. A. Cleugh, C. S. B. Grimmond, H. P. Schmid, and M. Roth, 1989: Evaluation of spatially averaged fluxes of heat, mass and momentum in the urban boundary layer. *Wea. Climate,* **9,** 14–21.

——, R. Spronken-Smith, E. Jauregui, and C. S. B. Grimmond, 1999: The energy balance of central Mexico City during the dry season. *Atmos. Environ.,* in press.

Roth, M., and T. R. Oke, 1994: Comparison of modeled and ''measured'' heat storage in suburban terrain. *Beitr. Phys. Atmos.,* **67,** 149–156.

Schmid, H. P., 1994: Source areas for scalars and scalar fluxes. *Bound.-Layer Meteor.,* **67,** 293–318.

——, 1997: Experimental design for flux measurements: Matching the scale of the observations to the scale of the flux. *Agric. For. Meteor.,* **87,** 179–200.

——, H. A. Cleugh, C. S. B. Grimmond, and T. R. Oke, 1991: Spatial variability of energy fluxes in suburban terrain. *Bound.-Layer Meteor.,* **54,** 249–276.

Souch, C., C. S. B. Grimmond, and C. Wolfe, 1998: Evaporation rates for wetlands with different disturbance histories: Indiana Dunes National Lakeshore. *Wetlands,* **18,** 216–229.

Steyn, D. G., 1985: An objective model to achieve closure of over determined surface energy budgets. *Bound.-Layer Meteor.,* **33,** 303–311.

Stull, R. B., 1988: *An Introduction to Boundary Layer Meteorology.* Kluwer Academic Publishers, 666 pp.

Taesler, R., 1980: Studies of the development and thermal structure of the urban boundary layer in Uppsala. Part I: Experimental Program; and Part II: Data, analysis and results. Rep. 61, Meteorological Institution, Uppsala University, Uppsala, Sweden, 236 pp. [Available from Department of Earth Sciences and Meteorology, Uppsala University Villavägen 16, S-752 36 Uppsala, Sweden.]

Taha, H., 1999: Modifying a mesoscale meteorological model to better incorporate urban heat storage: A bulk-parameterization approach. *J. Appl. Meteor.,* **38,** 466–473.

Tanner, B. D., and J. P. Greene, 1989: Measurements of sensible heat and water vapor fluxes using eddy correlation method. Final Report to U.S. Army Dugway Proving Grounds, 98 pp.

——, E. Swiatek, and J. P. Greene, 1993: Density fluctuations and use of krypton hygrometers in surface flux measurements. *Management of Irrigation and Drainage Systems,* ASCE, 945–952.

Webb, E. K., G. I. Pearman, and R. Leuning, 1980: Correction of flux measurements for density effects due to heat and water vapour transfer. *Quart. J. Roy. Meteor. Soc.,* **106,** 85–100.

Wyngaard, J., 1973: On surface layer turbulence. *Workshop on Micrometeorology,* D. A. Haugen, Ed., Amer. Meteor. Soc., 101–149.

Yap, D. H., 1973: Sensible heat fluxes in and near Vancouver, B.C. Ph.D. thesis, The University of British Columbia, Vancouver, Canada, 177 pp.

Yoshida, A., K. Tominaga, and S. Watatani, 1990–91: Field measurements on energy balance of an urban canyon in the summer season. *Energy Build.,* **15–16,** 417–423.